Rogue waves in nonlinear hyperbolic systems (shallow-water framework)

2011 Nonlinearity 24 R1

(http://iopscience.iop.org/0951-7715/24/3/R01)

IOP PUBLISHING NONLINEARITY

Nonlinearity **24** (2011) R1–R18 doi:10.1088/0951-7715/24/3/R01

INVITED ARTICLE

Rogue waves in nonlinear hyperbolic systems (shallow-water framework)*

Ira Didenkulova[1,2] **and Efim Pelinovsky**[2]

[1] Department of Applied Mathematics and Mechanics, Institute of Cybernetics, Tallinn University of Technology, Tallinn, Estonia
[2] Department of Nonlinear Geophysical Processes, Institute of Applied Physics, Nizhny Novgorod, Russia

Received 15 November 2010
Published 25 January 2011
Online at stacks.iop.org/Non/24/R1

Recommended by A I Neishtadt

Abstract

The formation of rogue waves is studied in the framework of nonlinear hyperbolic systems with an application to nonlinear shallow-water waves. It is shown that the nonlinearity in the random Riemann (travelling) wave, which manifests in the steeping of the face-front of the wave, does not lead to extreme wave formation. At the same time, the strongly nonlinear Riemann wave cannot be described by the Gaussian statistics for all components of the wave field. It is shown that rogue waves can appear in nonlinear hyperbolic systems only in the result of nonlinear wave–wave or/and wave–bottom interaction. Two special cases of wave interaction with a vertical wall (interaction of two Riemann waves propagating in opposite directions) and wave transformation in the basin of variable depth are studied in detail. Open problems of the rogue wave occurrence in nonlinear hyperbolic systems are discussed.

Mathematics Subject Classification: 35L70, 35L76, 35L86

(Some figures in this article are in colour only in the electronic version)

1. Introduction

Rogue waves in the ocean, whose height is two or more times greater than the typical wave background, have become very popular and have been actively studied over the last 20 years; see, for example, the following book and reviews (Kharif and Pelinovsky 2003, Dysthe *et al* 2008, Kharif *et al* 2009). The general study of rogue waves usually follows two directions. The first one is the statistical description of the nonlinear wave field based on the Gaussian distribution of the sea surface in the linear approximation (central limit theorem due to the large number of independent spectral components). It should be mentioned that distribution of

* This invited article is one of a series published throughout 2011 in *Nonlinearity* on the topic of Rogue Waves.

extremes in general is a hard mathematical task even for a Gaussian sea (Machado and Rychlik 2003, Baxevani and Rychlik 2006) with the exception of the narrow-band wind wave process, when the extremes are distributed by the Rayleigh law (Kharif *et al* 2009). It is known that nonlinearity leads to the correlation of the spectral components and non-Gaussianity of the wave field (Dysthe *et al* 2008). The most famous examples of this effect are Stokes waves in deep water and cnoidal waves and solitons in shallow water. This effect is manifested in the development of sharp and pointed wave crests and long and gentle troughs. As a result, the distribution of the wave crests differs from the distribution of wave troughs in the nonlinear theory (Dysthe *et al* 2008).

Another approach is aimed at studying physical mechanisms of rogue wave generation in the ocean (Kharif *et al* 2009). Modern theory considers several basic mechanisms. First of all, these are the focusing effects caused by geometry of the wave front (the lens's effect), wave dispersion (dispersive focusing) and wave–bottom and wave–current interaction. Of course, all these mechanisms are valid in linear theory as well, but nonlinearity makes its principal contribution on the structure of wave field in singular points (focuses and caustics). A second group of rogue wave generation mechanisms is connected to nonlinear wave interaction and instability. For instance, the oblique soliton interaction in the framework of the Kadomtsev–Petviashvilli (KP) equation may lead to the four-time amplification of the wave field (Soomere 2010, Yeh *et al* 2010). One of the most popular models demonstrating modulation or Benjamin–Feir instability is the nonlinear Schrodinger equation, which is fully integrable in mathematical physics (Zakharov and Ostrovsky 2009). This modulation instability leads to the appearance of short-lived groups of high-amplitude waves (breathers), where amplitude may exceed the amplitude of the wave background by up to three times (Peregrine 1983, Dysthe and Trulsen 1999, Akhmediev *et al* 2009b). In the framework of the nonlinear Schrodinger equation the breather and wave packets interaction can lead to the generation of super rogue waves (Kharif *et al* 2001, Onorato *et al* 2001, Akhmediev *et al* 2009a). The breather solution has recently found to be numerically within fully nonlinear equations of water waves (Dyachenko and Zakharov 2005, 2008, Slunyaev 2009).

The third group of mechanisms of the rogue wave generation in the ocean is related to external factors: wind flow above the water surface and bottom friction; most of the results here are obtained numerically (Kharif *et al* 2008, Voronovich *et al* 2008). Appropriate models for the description of these effects are forced nonlinear evolution equations, for example, the forced Korteweg–de Vries equation.

Four years ago the rogue wave phenomenon was discovered in nonlinear optical fibres (Solli *et al* 2007) and then in other nonlinear systems: superfluid helium, laboratory and space plasma, Bose–Einstein condensates and geophysical flows, see, for example, Ruban *et al* (2010) and other papers in this special issue. The most popular model, used in all these problems, is the nonlinear Schrodinger equation and its generalizations. The main physical mechanism in this case is modulation instability. That is why modulation instability is considered as a major factor of the rogue wave appearance in all branches of physics. In particular, for unidirectional water wave propagation the modulation instability occurs for $kh > 1.36$, where k is the wave number, h is the water depth.

Nevertheless, numerous eye-witness observations and coastal sea level records demonstrate that rogue waves also occur in shallow water, where modulation instability becomes weak. Therefore, we can expect that the main contribution to rogue wave formation in shallow water is given by the first group of mechanisms: geometrical and dispersive focusing, wave–bottom and wave–current interaction.

In nearshore water waves can be considered as long waves (their wavelength is much greater than the water depth due to decreasing water depth near the coast) and, therefore, the

Figure 1. Freak waves in Mavericks Beach (California, USA) on 14 February 2010 (© Scott Anderson).

basic mathematical model may be a hyperbolic system of nonlinear shallow-water equations or its weakly dispersive generalizations (KdV, KP and Bousinesq equations). This paper aims to describe the rogue wave phenomenon in the 1 + 1 hyperbolic system for nonlinear water waves.

The paper is organized as follows. Manifestations of coastal rogue waves are presented in section 2. The 1 + 1 hyperbolic system and its Riemann invariants for nonlinear water waves in inclined channels of various cross-sections are discussed in section 3. The statistics of Riemann waves propagating in the channel of constant cross-section is analysed in section 4. The interaction of two Riemann waves propagating in opposite directions and wave–wall interaction is studied in section 5. Nonlinear wave shoaling and runup in the inclined channel is considered in section 6. The main results are summarized in the conclusion.

2. Rogue waves in the coastal zone: observations and records

Rogue events occurring onshore usually result in a short-time sudden flooding of the coast (figure 1) or strong impact upon a steep bank or coastal structure (figure 2). Descriptions of such accidents are given in Dean and Dalrymple (2002) and Kharif *et al* (2009). They frequently lead to damage of coastal structures and loss of lives. Chien *et al* (2002) reports about 140 rogue wave events in the coastal zone of Taiwan in the past 50 years (1949–1999), because of which more than 496 people lost their lives and more than 35 crafts were capsized. Didenkulova *et al* (2006) collected and analysed information about rogue wave accidents, reported by the mass media in 2005. Nine cases were selected as true rogue wave events, from which six occurred nearshore. Two of the very recent events occurred on 14 February 2010 in Mavericks Beach in California, USA, when two unexpected 6 m high waves washed off 13 people standing on the parapet at the coast (figure 1) and on 7 March 2010 in Kristiansund, Norway, when two 9-year old girls were killed by a rogue wave. A similar phenomenon was noticed in Cassis, France, on 26 June 2010 when suddenly four unexpectedly high waves attacked the coast and washed away a lot of people's belongings.

A peculiar rogue wave was observed on Kamchatka coast, Russia, on 11 June 2006 (figure 3). The 4 m wave appeared suddenly, propagated about 50 m and collapsed during tens of seconds. A similar wave was seen at the Sakhalin coast of Russia on 2 August 2010. Observations of such events become more frequent, and they broaden the area of possible freak wave occurrence.

Rogue waves in the coastal zone have a strongly nonlinear character due to decreasing water depth, but manifestations of this nonlinearity can be different. Figure 1 demonstrates

Figure 2. Wave impact on the steep rock bank on Sotra, Norway on 26 December 2007.

Figure 3. The wave near Kamchatka coast, Russia, on 11 June 2006 (© Mstislav Sokolovsky). Two different viewing angles of the same wave.

the turbulent structure of the climbing beach flow. Figure 2 displays a vertical wave splash on a rock and figure 3 shows the 2D wave of an asymmetric shape.

The asymmetric shape of the wave by means of face-back slope asymmetry has often been observed in the recorded time-series as well. Figures 4 and 5 show the rogue waves of both positive and negative polarity, recorded in the coastal zone of the Baltic Sea, at the depth 2.7 m (Didenkulova and Anderson 2010, Didenkulova 2011). Both waves have a clearly identified asymmetric front and significantly exceed all other neighbouring waves.

Examples of rogue waves nearshore demonstrate the important role of nonlinearity in their formation and nonlinear theory is required for their description.

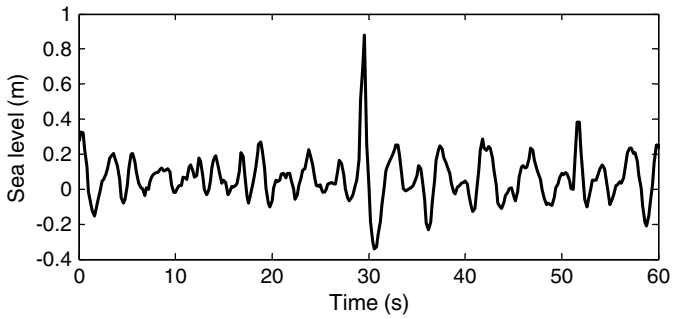

Figure 4. Rogue wave of a positive shape on 9 July 2008 in the Baltic Sea, depth 2.7 m.

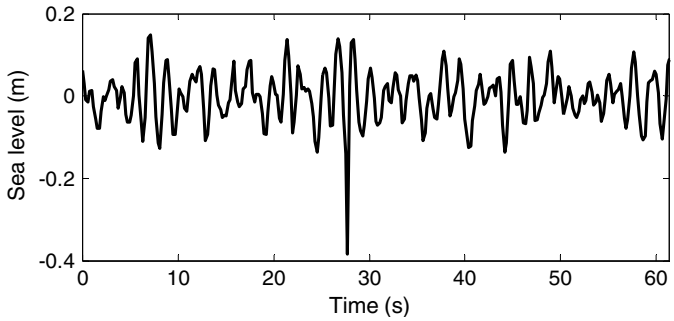

Figure 5. Rogue wave of a negative shape on 19 July 2008 in the Baltic Sea, depth 2.7 m.

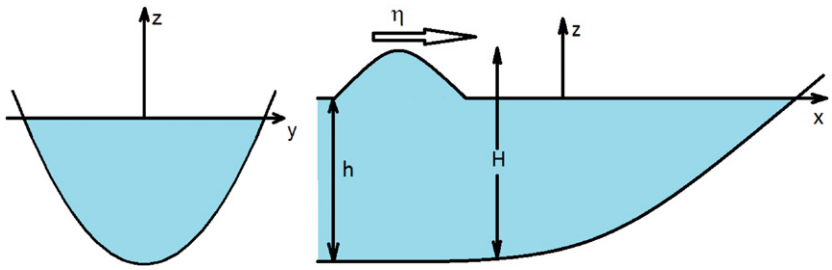

Figure 6. Cross-section and longitudinal projection of the bay.

3. Nonlinear hyperbolic equations for water waves in channels

As a characteristic example of rogue waves in nonlinear hyperbolic equations, let us consider rogue wave phenomenon in water channels of arbitrary longitudinal and transversal projections (figure 6). In this case the basic equations describing the dynamics of long nonlinear waves are nonlinear shallow-water equations, which represent the mass (continuity) and momentum conservation along the channel axis

$$\frac{\partial S}{\partial t} + \frac{\partial}{\partial x}(Su) = 0, \qquad \frac{\partial u}{\partial t} + u\frac{\partial u}{\partial x} + g\frac{\partial H}{\partial x} = g\frac{\mathrm{d}h}{\mathrm{d}x}, \tag{1}$$

where $S(x,t)$ is the water-filled cross-section area of the channel, $H(x,t) = h(x) + \eta(x,t)$ is the total depth along the main channel axis (positive-definite function), $h(x)$ is an unperturbed

water depth along the channel axis, $\eta(x, t)$ is the water surface displacement and $u(x, t)$ is the flow velocity averaged over the cross-section. System (1) can be closed taking into account the specific shape of the channel cross-section. If we assume that the channel topography is described by

$$z(x, y) = -h(x) + f(y), \tag{2}$$

where f is a symmetric function $f(y) = f(-y)$ describing the cross-section geometry, which has its minimum at the channel axis and increases to both sides, and does not depend on the horizontal coordinate x, then

$$S = S(H), \tag{3}$$

and system (1) becomes closed.

Equations (1) together with equation (3) represent the nonlinear hyperbolic system with an external forcing $(\mathrm{d}h/\mathrm{d}x)$. The boundary conditions for this system depend on $h(x)$. If $h(x)$ is a gradually increasing function, the kinematic boundary condition is given at the unknown moving boundary:

$$H(x, t) = 0. \tag{4}$$

This situation is realized in narrow bays and fjords, where the moving boundary is represented by the moving shoreline.

Another boundary condition should describe the incident wave entering the channel (it will be discussed later). In the context of rogue wave phenomenon the incident wave represents the random function with known statistics. Initial conditions can be assumed to be zero.

Thus, in general, we should solve the nonlinear hyperbolic system in the domain with one unknown moving boundary (the moving shoreline) and random input defined at the opposite side of the domain (the open sea). In sections 4, 5 and 6 we consider three special cases that allow rigorous analytical analysis of the random nonlinear wave field.

4. Riemann waves and their statistics

It is natural to start with the case of nonlinear wave propagation in the basin with $h(x) = \text{const}$. Due to the hyperbolic character of the system the travelling wave solution of equations (1) has a form of the Riemann wave (Stoker 1957, Engelbrecht *et al* 1988, Zahibo *et al* 2008). In this case we should assume $u = u(H)$ or $u = u(\eta)$ and the required compatibility condition for equations leads to the following relation between the velocity u and the water level η:

$$u(\eta) = \pm \int_h^{h+\eta} \sqrt{\frac{g}{S}\frac{\mathrm{d}S}{\mathrm{d}\zeta}}\,\mathrm{d}\zeta, \tag{5}$$

where the sign $+/-$ corresponds to the wave propagating in right/left direction along the x-axis. Let us consider the wave propagating to the right here. Substituting equation (5) into any equation of system (1), we have one equation for the water displacement

$$\frac{\partial \eta}{\partial t} + V(h, \eta)\frac{\partial \eta}{\partial x} = 0, \tag{6}$$

where the nonlinear speed of the wave propagation is

$$V(h, \eta) = \sqrt{\frac{gS}{\mathrm{d}S/\mathrm{d}\zeta\,|_{\zeta=h+\eta}}} + \int_h^{h+\eta} \sqrt{\frac{g}{S}\frac{\mathrm{d}S}{\mathrm{d}\zeta}}\,\mathrm{d}\zeta. \tag{7}$$

The first-order equation (6) can be solved analytically, and its solution satisfying the boundary condition $\eta(x_0, t) = \eta_0(t)$ represents the simple (Riemann) wave

$$\eta(x, t) = \eta_0\left(t - \frac{x - x_0}{V(h, \eta)}\right). \tag{8}$$

The shape of the boundary function $\eta_0(t)$ can be arbitrary in the space L^2. Taking into account physical applications of the obtained solutions we may assume that the incident wave has a smooth shape and can be presented by the convergent Fourier series with the random phase of spectral components. This approach is very popular in the modelling of random wave phenomena.

The nonlinear deformation of the Riemann wave is manifested in its front, which becomes steeper with the distance, and finally transforms into a shock wave (bore). This can also be confirmed by the direct calculation of the face-slope wave steepness. The steepness of the wave profile in time-series can be found from equation (8):

$$\frac{\partial \eta}{\partial t} = \frac{\mathrm{d}\eta_0/\mathrm{d}t}{1 + (x - x_0)(\mathrm{d}V^{-1}/\mathrm{d}\eta)(\mathrm{d}\eta_0/\mathrm{d}t)}, \tag{9}$$

and it tends to infinity at the 'breaking length'

$$L = \frac{1}{\max(-(\mathrm{d}V^{-1}/\mathrm{d}\eta)(\mathrm{d}\eta_0/\mathrm{d}t))}. \tag{10}$$

For demonstration of the effect of wave deformation we consider the 'power' approximation of the channel walls

$$h(y) = b|y/y_0|^m, \tag{11}$$

where coefficients b and m are positive and y_0 is the effective width of the channel. In this case the nonlinear and linear speeds of wave propagation in the channel are

$$V(h, \eta) = 2\sqrt{\frac{m+1}{m}}(\sqrt{g(h+\eta)} - \sqrt{gh}) + \sqrt{\frac{m}{1+m}}\sqrt{g(h+\eta)}, \tag{12}$$

$$c = V(h, \eta = 0) = \sqrt{\frac{m}{1+m}gh}. \tag{13}$$

In the limit of the rectangular channel ($m \to \infty$) $c = \sqrt{gh}$. The nonlinearity leads to the increase in speed for wave elevations (crests) and decrease in speed for wave depressions (troughs). As a result, the wave front becomes steeper (figure 7).

It is important to mention that the nonlinear speed of wave deformation can be negative for large-amplitude wave troughs and the critical depth, when $V = 0$, is

$$H_{\mathrm{cr}} = 4\left(\frac{m+1}{3m+2}\right)^2 h_0. \tag{14}$$

In the case of rectangular basin the critical depth is $H_{\mathrm{cr}} = 4h_0/9$ (Zahibo *et al* 2008). When m decreases, the critical depth tends to h_0 (figure 8). Surprisingly, large-amplitude wave troughs move to the left and, therefore, cannot be in the domain $x > x_0$, where we solve the boundary problem. At the same time we assume that the nonlinear wave propagates to the right. This paradox can be resolved by the analysis of the breaking length (10) that shows that large-amplitude waves break in the vicinity of the $x = x_0$. It means that the correct solution of the boundary problem for hyperbolic equations (1) can be given only for initially smooth disturbances with an additional condition to 'negative' wave amplitudes: $H > -H_{\mathrm{cr}}$.

The velocity field in the Riemann wave is described by equation (5). In the case of the channel with the 'power' cross-section it is

$$u(\eta) = 2\sqrt{\frac{m+1}{m}}(\sqrt{g(h+\eta)} - \sqrt{gh}). \tag{15}$$

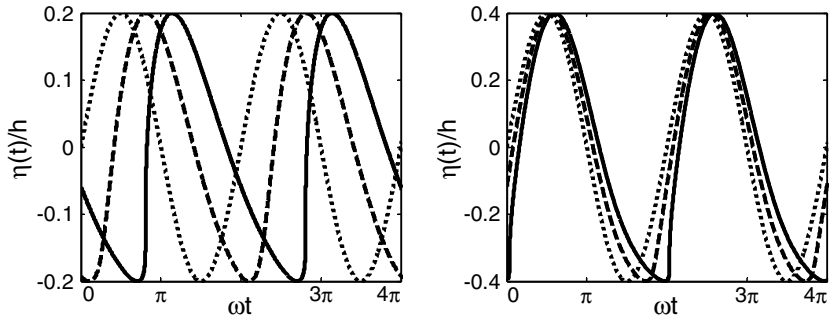

Figure 7. Nonlinear transformation of a sine wave with distance $x = 0$ (dotted), $L/2$ (dashed) and L (solid line).

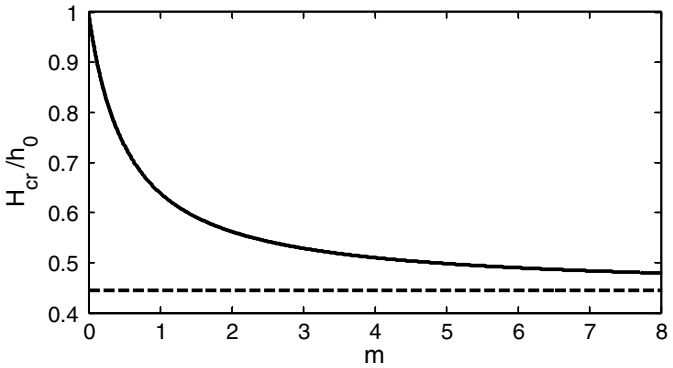

Figure 8. The critical depth (solid line), $H_{\rm cr}/h_0 = 4/9$ (dashed line).

It follows from equation (15) that the velocity is positive under the wave crest and negative under the trough. In fact, the appropriate nonlinear parameter here is the Mach number that is the ratio of the flow velocity (15) and the wave speed (12). It varies from zero in the linear limit to infinity (considering absolute value of the ratio) demonstrating a strongly nonlinear character of Riemann waves in water channels.

Description of the process of the wave breaking even for shallow-water waves is a hard mathematical task. As it is known (Stoker 1957) a large-amplitude long wave can develop into a typical shock wave (bore), while a weak-amplitude long wave may transform into an undular bore or a set of solitons. The mathematical description of the water wave breaking process is an open problem (Pomeau *et al* 2008), which is not discussed here.

The approach described above is usually used for deterministic incident waves, while it can also be applied to the random wave field. Such processes have actively been studied in nonlinear acoustics for narrow-band signals (Rudenko and Soluyan 1977). In this case the statistical analysis of various characteristics of the wave field (the breaking length, intensities of generated super- and sub-harmonics, etc) can be performed. Some rigorous analytical results have been obtained for random Riemann waves (Gurbatov *et al* 1991). In particular, if the incident wave field represents the stationary random process, its probability distribution does not vary with distance (of course, if the wave breaking can be neglected). Physically, it is understandable, since each local point of the wave profile moves with its own speed and does not change in amplitude, hence the number of local points with close amplitudes in the Riemann wave conserves.

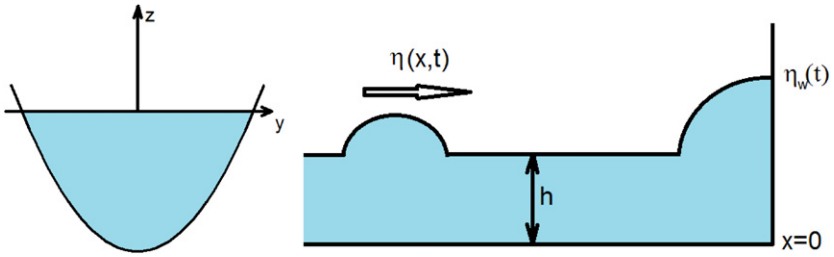

Figure 9. The geometry of the problem.

Very often the Gaussian distribution is used for description of the random wave field in nonlinear acoustics. For the weakly nonlinear acoustical signals both water displacement and particle velocity can represent Gaussian processes, while for strongly nonlinear Riemann waves due to equation (15) both wave characteristics cannot be described by the same distribution. In this case if the water displacement is the Gaussian process then the particle velocity cannot be described by the Gaussian process and vice versa. Their probability density functions W are related by

$$W(u) = W(\eta)|\mathrm{d}\eta/\mathrm{d}u|. \tag{16}$$

Going back to the rogue wave phenomenon we should conclude that the probability of the appearance of high-amplitude picks in the Riemann wave field does not change with the distance, and nonlinear deformation of shallow-water waves does not influence on the statistics of extreme waves. Of course, wave breaking may change the probability distribution significantly, but it is outside of the Riemann wave approximation.

5. Riemann wave interaction with the wall

The nonlinear interaction of Riemann waves cardinally changes the statistics of the wave field in hyperbolic systems. Let us consider the interaction of two waves of the same shape propagating in opposite directions in the channel of constant depth along the longitudinal direction. In the water wave application this situation usually occurs, when the wave approaches the steep coast (cliff) or the seawall, which is used for protection of population and coastal structures against high waves (figure 9).

In this case, from the mathematical point of view system (1) with $h(x) = \text{const}$ should be solved with the following boundary condition at the wall $x = 0$:

$$u(x = 0, t) = 0, \tag{17}$$

which indicates that there is no water penetration through the wall. Taking into account the hyperbolic type of system (1), it is convenient to re-determine Riemann invariants

$$I_{\pm} = u \pm \int_h^H \sqrt{\frac{g}{S}\frac{\mathrm{d}S}{\mathrm{d}\zeta}}\,\mathrm{d}\zeta, \tag{18}$$

assuming that invariants are zero for the calm sea state, when there is no wave motion, and to rewrite equations (1) in the form

$$\frac{\partial I_{\pm}}{\partial t} + V_{\pm}\frac{\partial I_{\pm}}{\partial x} = 0, \tag{19}$$

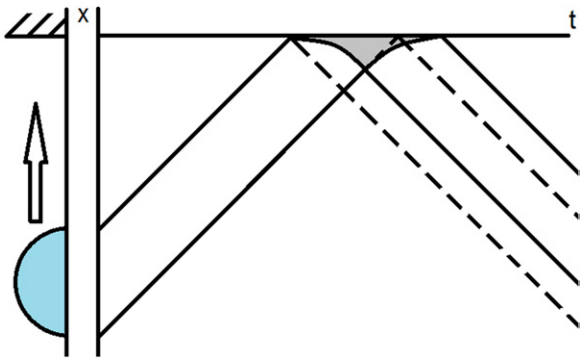

Figure 10. Characteristics of the interaction between the incident and reflected waves.

where the characteristic speeds are

$$V_{\pm} = u \pm \sqrt{\frac{gS}{\mathrm{d}S/\mathrm{d}H}}. \tag{20}$$

It follows from equation (19) that $I_{\pm}$ do not change along characteristics $V_{\pm}$. Let us study the wave–wall interaction for the case when an incident wave approaching the wall from $x < 0$ has a finite duration first (figure 10). As it is known and also follows from equation (19) the characteristics $V_{\pm}$ represent straight parallel lines in the linear theory framework (dashed lines in figure 10). In the nonlinear theory framework the characteristic speeds $V_{\pm}$ depend on the wave field, therefore, they can be presented as straight non-parallel lines only outside of the near-wall interaction domain (figure 10). Inside the interaction domain characteristics bend, as shown in figure 10. Since Riemann invariants do not change along the characteristics, the nonlinear interaction reduces to the additional phase shift between waves. For the incident wave defined at any location from the wall $I_{-} = 0$ and I_{+} is determined by

$$I_{+}(\eta_{\mathrm{in}}) = 2\int_{h}^{h+\eta_{\mathrm{in}}} \sqrt{\frac{g}{S}\frac{\mathrm{d}S}{\mathrm{d}\zeta}}\,\mathrm{d}\zeta. \tag{21}$$

At the wall due to the boundary condition (17) the same Riemann invariant is

$$I_{+}(\eta_{\mathrm{w}}) = \int_{h}^{h+\eta_{\mathrm{w}}} \sqrt{\frac{g}{S}\frac{\mathrm{d}S}{\mathrm{d}\zeta}}\,\mathrm{d}\zeta. \tag{22}$$

Equating equations (21) and (22) we can find the integral relation between the water displacement at the wall η_{w} and the incident wave η_{in}:

$$\int_{h}^{h+\eta_{\mathrm{w}}} \sqrt{\frac{g}{S}\frac{\mathrm{d}S}{\mathrm{d}\zeta}}\mathrm{d}\zeta = 2\int_{h}^{h+\eta_{\mathrm{in}}} \sqrt{\frac{g}{S}\frac{\mathrm{d}S}{\mathrm{d}\zeta}}\,\mathrm{d}\zeta. \tag{23}$$

As a result, sea level oscillations at the wall can be expressed through the water displacement in the incident wave. Unfortunately, this method does not predict the time shift τ between two functions, which is generally the unknown functional of the wave field in the interaction zone. That is why it is hard to use equation (23) for calculations of time-series of near-wall sea level oscillations even for known characteristics of the incident wave. Meanwhile, there is one practical consequence that follows from equation (23) if we consider the extreme values of the wave field far offshore and at the wall:

$$\int_{h}^{H_w} \sqrt{\frac{g}{S}\frac{\mathrm{d}S}{\mathrm{d}\zeta}}\,\mathrm{d}\zeta = 2\int_{h}^{H_{\mathrm{in}}} \sqrt{\frac{g}{S}\frac{\mathrm{d}S}{\mathrm{d}\zeta}}\,\mathrm{d}\zeta, \tag{24}$$

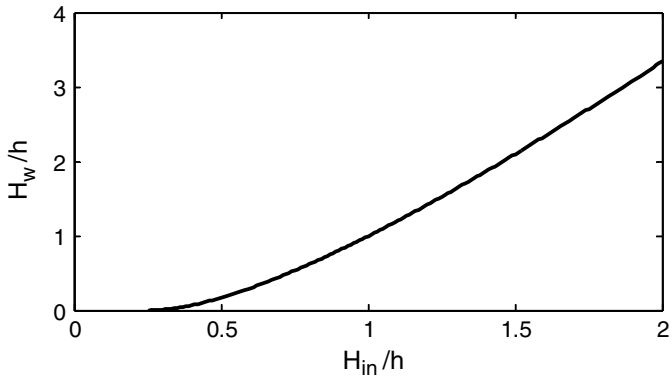

Figure 11. Relation between extreme values of the water flow far offshore and at the wall.

where H_{in} and H_{w} are extreme values of the total depth (depth of water flow) far offshore and at the wall, respectively, which are usually used for the estimate of the wave impact on the wall.

Let us consider again the channel of the 'power' cross-section (11). In this case the integrals in equation (24) can be found analytically:

$$\frac{H_{\mathrm{w}}}{h} = 1 + 4\left[\frac{H_{\mathrm{in}}}{h} - \sqrt{\frac{H_{\mathrm{in}}}{h}}\right]. \tag{25}$$

Surprisingly, equation (25) does not depend on the shape of the channel cross-section and is the same for 'power' and rectangular type of the channel (figure 11). This expression for the rectangular channel was found in Pelinovsky (1995) and Pelinovsky *et al* (2008).

Since an incident and reflected waves can always be separated in space, this approach can also be applied to the irregular wave field. In this case, it can be used to analyse distribution functions of the wave field and its spectrum. Unfortunately, as it has been pointed out above, it cannot predict the time shift between the incident field and water oscillations at the wall, and, therefore, the function $\eta_{\mathrm{w}}(t)$ is not fully determined within the nonlinear shallow-water theory framework. Hence, the water level distribution at the wall cannot be found even if the statistics of the incident wave is known. At the same time, the obtained relation between the extremes of the incident water flow and the flow depth at the wall equation (25) does not include the time shift. As a result using equation (25) we can find the distribution of the extreme water oscillations at the wall by knowing the distribution function of the extremes of the incident water flow field. In this case the probability density function can be expressed similar to equation (16):

$$W_{H_{\mathrm{w}}}(H_{\mathrm{w}}) = W_{H_{\mathrm{in}}}(H_{\mathrm{in}}) \left|\frac{\mathrm{d}H_{\mathrm{in}}}{\mathrm{d}H_{\mathrm{w}}}\right|\Bigg|_{H_{\mathrm{in}}(H_{\mathrm{w}})}. \tag{26}$$

The exceedance probability of water extremes can be found by integrating the probability density function equation (26). If we assume that the distribution of the incident wave amplitudes (extreme values of the total depth) are described by the Rayleigh distribution, which is usually used in statistical theory of linear narrow-band wind waves (Kharif *et al* 2009):

$$P(H_{\mathrm{in}}) = \exp\left(-\frac{2(H_{\mathrm{in}} - h)^2}{A_{\mathrm{s}}^2}\right), \tag{27}$$

where A_{s} is the so-called significant wave amplitude, which is determined as 2σ for the Gaussian process, where σ is a standard deviation, the exceedance probability of water extremes

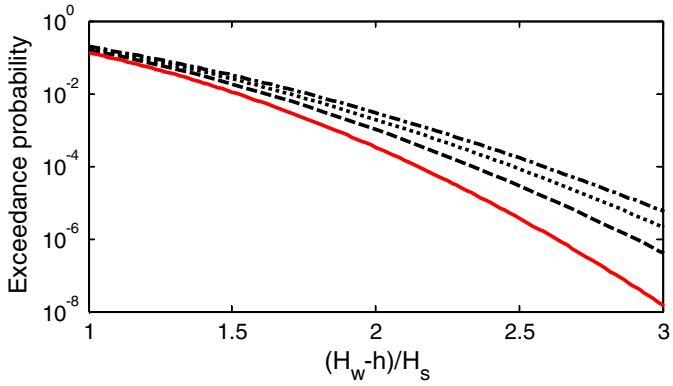

Figure 12. The exceedance probability function of extreme water oscillations at the wall for different values of the parameter $\varepsilon = 0.2$ (dashed), 0.4 (dotted) and 0.6 (dashed–dotted line); the solid line corresponds to the Rayleigh distribution.

at the wall can be calculated and is presented in figure 12 for different values of the parameter $\varepsilon = H_s/h$, where $H_s = 2A_s$ (the significant wave height at the wall is twice as large as far offshore in the linear theory).

It can be seen that nonlinearity increases the probability of the appearance of high water at the wall, and, therefore, rogue waves appear more frequently at the coast than in the open sea. It may explain why the accidents caused by unusual and short-lived overtopping of breakwaters described in section 2 occur so often. Another physical effect, which has a major importance for large-amplitude waves, is the wave breaking. Taking it into account in the study of freak wave formation at the wall and coastal structures remains an open problem.

6. Runup of random waves in inclined channels

If the depth along channel axes is varied, the rigorous analytical solution of the nonlinear system (1) is known only for the case when the function $h(x)$ is linear, and only for specific cross-sections of the channel. In this case, the linearly inclined bottom profile along the channel allows wave propagation and runup to the dry beach. This mathematical problem is extremely important in the context of coastal engineering since it allows the calculation of wave heights on a beach, the inundation level, and waving impact on coasts and coastal constructions.

If we fix $h(x) = \alpha x$, the 'forced' term in equations (1) can be removed by the transformation

$$u(x,t) = g\alpha t + v(x,t), \qquad x' = x - g\alpha t^2/2, \tag{28}$$

and the new system takes the following form

$$\frac{\partial S}{\partial t} + \frac{\partial}{\partial x'}(Sv) = 0, \qquad \frac{\partial v}{\partial t} + v\frac{\partial v}{\partial x'} + g\frac{\partial H}{\partial x'} = 0. \tag{29}$$

As it has been demonstrated in the previous section, equations (29) can be rewritten through Riemann invariants (18):

$$\frac{\partial I_\pm}{\partial t} + V_\pm \frac{\partial I_\pm}{\partial x'} = 0, \qquad V_\pm = v \pm \sqrt{\frac{gS}{\mathrm{d}S/\mathrm{d}H}}. \tag{30}$$

An effective approach of solving nonlinear equations is a hodograph transformation, which suggests using x' and t as functions and I_+ and I_- as arguments. If we consider again the

inclined channel with the 'power' cross-section, the solution of the nonlinear system (1) can be expressed in terms of the initial physical variables (see Zahibo *et al* (2006) for details):

$$\frac{\partial^2\Phi}{\partial\lambda^2} - \frac{\partial^2\Phi}{\partial\sigma^2} - \frac{(m+2)}{m\sigma}\frac{\partial\Phi}{\partial\sigma} = 0, \tag{31}$$

$$\eta = \frac{1}{2g}\left[\frac{m}{(m+1)}\frac{\partial\Phi}{\partial\lambda} - u^2\right], \qquad H = \frac{m}{(m+1)}\frac{\sigma^2}{4g}, \qquad u = \frac{1}{\sigma}\frac{\partial\Phi}{\partial\sigma}, \tag{32}$$

$$x = \frac{\eta}{\alpha} - \frac{m\sigma^2}{4g\alpha(m+1)}, \qquad t = \frac{\lambda - u}{g\alpha}. \tag{33}$$

As a result, the initial system of nonlinear shallow-water equations (1) has been reduced to the linear wave equation (31) and all physical variables can be found from Φ. The main advantage of this form is that the moving (unknown) boundary (the shoreline) corresponds to the fixed value of $\sigma = 0$ (the total depth $H = 0$ from equation (32)) and, therefore, equation (31) is solved in the half-space $0 < \sigma < \infty$ with the fixed boundary. This transformation has first been suggested for waves climbing the plane beach (Carrier and Greenspan 1958), and then has been generalized for the inclined channels (Zahibo *et al* 2006, Choi *et al* 2008, Didenkulova and Pelinovsky 2009).

Since the channel has a 2D geometry, we need to specify the location of the moving boundary (the shoreline) across the channel axis. From equation (11) it follows that

$$y(x,t) = \frac{H^{1/m}(x,t)}{b^{1/m}} y_0 \sim \sigma^{2/m}. \tag{34}$$

The wave equation (31) defined on the semi-axis is well studied in mathematical physics. In particular, for a plane beach or rectangular channel it reduces to the radial cylindrical wave equation and for the channel of a parabolic shape ($m = 2$)—to the radial spherical wave equation. Both equations have been used to study wave runup on a beach including the runup of the Korteweg–de Vries (KdV) soliton (Synolakis 1987, Choi *et al* 2008). At the same time the initial conditions for equation (31) are not so trivial. General initial conditions for the physical wave field (the water displacement and flow velocity) transform to the conditions on the function Φ and $\partial\Phi/\partial\lambda$ along the line $\lambda(\sigma)$, which can be complicated. Only in the case when the initial velocity is zero (a so-called 'piston' model for tsunami wave generation), are the initial conditions for equation (31) determined in the point $\lambda = 0$ and correspond to the 'standard' initial conditions for wave equation. An attempt to study the runup problem with non-zero initial condition for the flow velocity was made by Kânoğlu and Synolakis (2006) and still remains an open problem.

Boundary conditions for equation (31) naturally correspond to the boundedness of the function Φ and its derivative in the point of the moving shoreline $\sigma = 0$, and the Sommerfeld radiation condition at infinity.

In the following we do not discuss the specific features of solving the initial or boundary problem for equation (31), but focus on the nonlinear dynamics of the moving shoreline ($\sigma = 0$) only. From the last equation in (33) we get the implicit expression for the velocity of the moving shoreline $u = u(\lambda, \sigma = 0) = u(g\alpha t + u)$, which can be rewritten in a more elegant form

$$u(t) = U\left(t + \frac{u}{\alpha g}\right), \tag{35}$$

where U has a physical sense of the shoreline velocity computed in the linear approximation. If we consider the incident wave given far from the shoreline where all nonlinear terms can be neglected, this function U can be easily found from the linear shallow-water equation and

expressed in terms of the parameters of the incident wave. In a similar way we can express the vertical displacement of the moving shoreline along the main channel axis

$$r(t) = \eta(\lambda, \sigma = 0) = R\left(t + \frac{u}{\alpha g}\right) - \frac{u^2}{2g}, \tag{36}$$

through the vertical water displacement $R(t)$ at the unperturbed shoreline ($x = 0$) found in the linear approximation.

Both pairs of variables, 'linear' (R and U) and 'nonlinear' (r and u), are also connected to each other since the velocity (u or U) represents the time derivative of the water displacement (r or R), divided by the bottom slope (it is clear from the geometry). So, a simplified way to study the nonlinear dynamics of the moving shoreline is to solve the linear shallow-water equations first and find the vertical water displacement in the point $x = 0$ and then to find 'real' (nonlinear) characteristics of the moving shoreline using equations (35) and (36).

The described approach is general and can be applied to regular and irregular initial conditions. With an application to the rogue wave phenomenon we assume that the incident wave field (given far from the shoreline where the waves are linear) represents the Gaussian stationary random process. In this case the functions $R(t)$ and $U(t)$ are also the random functions with Gaussian statistics, and do not correlate with each other. The nonlinearity in equations (35) and (36) is manifested by the transformation of time and in the additional term in equation (36). The velocity of the moving shoreline represents the 'frozen' Riemann wave (8), and can be described by the same Gaussian statistics. The function $r(t)$ is more complicated. On the one hand, it is an integral of $u(t)$, which usually represents a non-stationary process with the Brownian diffusion. On the other hand, it is described by equation (36), which contains the nonlinear quadratic term u^2, and should lead to the non-Gaussianity of the process. It is shown in Didenkulova *et al* (2011) that the function $r(t)$ represents the stationary non-Gaussian process. Finding the distribution function of the vertical shoreline displacement described by equation (36) still remains an open problem, but its statistical moments can be found explicitly.

Here we calculate statistical moments of the displacement of the moving shoreline, assuming the process to be ergodic and using time averaging. For example, the first moment is

$$\langle r \rangle = \frac{1}{T}\int_0^T R\left(t + \frac{u}{g\alpha}\right) \mathrm{d}t - \frac{\langle u^2 \rangle}{2g}, \tag{37}$$

where T is the time of the record (the length of the realization). It is also convenient to introduce a new variable

$$\tau = t + \frac{u(t)}{\alpha g}. \tag{38}$$

In this case

$$\mathrm{d}\tau = \mathrm{d}t\left[1 + \frac{1}{\alpha g}\frac{\mathrm{d}u}{\mathrm{d}t}\right], \tag{39}$$

and $\mathrm{d}u/\mathrm{d}t$ in equation (39) can be found exactly from equation (35)

$$\frac{\mathrm{d}u}{\mathrm{d}t} = \frac{\mathrm{d}U/\mathrm{d}\tau}{1 - (g\alpha)^{-1}\mathrm{d}U/\mathrm{d}\tau}. \tag{40}$$

Substituting equation (40) into equation (39) gives us the final expression for $\mathrm{d}t$

$$\mathrm{d}t = \left\lfloor 1 - (g\alpha)^{-1}\mathrm{d}U/\mathrm{d}\tau \right\rfloor \mathrm{d}\tau, \tag{41}$$

and integral (37) becomes explicit

$$\langle r \rangle = \frac{1}{T}\int_0^T R(\tau)\,\mathrm{d}\tau - \frac{1}{g\alpha T}\int_0^T R(\tau)\frac{\mathrm{d}U}{\mathrm{d}\tau}\mathrm{d}\tau - \frac{\langle U^2 \rangle}{2g}. \tag{42}$$

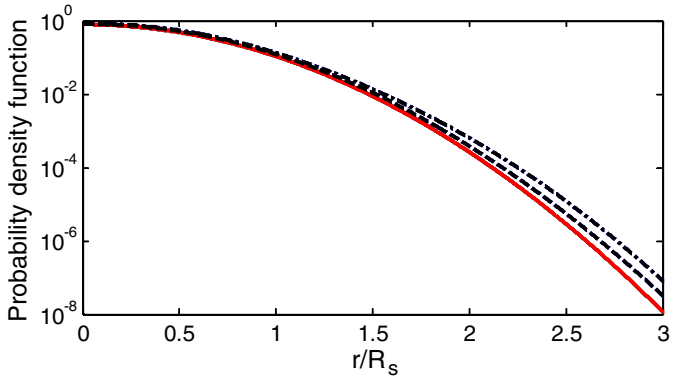

Figure 13. Probability density function of the displacement of the moving shoreline for $B = 0$ (solid line), 0.3 (dashed line) and 0.6 (dashed–dotted line).

Since $R(t)$ is defined with respect to the mean sea level and the mean sea level is constant in linear theory, we can assume it to be zero (the first term in equation (42)), hence the final expression for the mean displacement of the moving shoreline is

$$\langle r \rangle = \frac{\langle U^2 \rangle}{2g}. \tag{43}$$

It follows from equation (43) that the nonlinearity leads to an increase in the mean sea level at the coast (set-up) for any distribution of the wave field.

Omitting mathematical manipulations and again using assumptions of the Gaussian stationary process for the incident wave field we can write expressions for the standard deviation σ_r, skewness s and kurtosis k of the displacement of the moving shoreline, which can be presented in terms of the standard deviation in the linear theory σ_R:

$$\sigma_r^2 = \langle r^2 \rangle - \langle r \rangle^2 = \sigma_R^2 - 2\langle r \rangle^2, \tag{44}$$

$$s = \frac{\langle (r - \langle r \rangle)^3 \rangle}{\sigma_r^3} = \frac{8\langle r \rangle^3}{(\sigma_R^2 - 2\langle r \rangle^2)^{3/2}}, \tag{45}$$

$$k = \frac{\langle (r - \langle r \rangle)^4 \rangle}{\sigma_r^4} - 3 = \frac{\langle r \rangle^2 (4\sigma_R^2 - 23\langle r \rangle^2)}{(\sigma_R^2 - 2\langle r \rangle^2)^2}. \tag{46}$$

Equations (45) and (46) demonstrate that the vertical displacement of the moving shoreline differs from the Gaussian distribution. If this deviation is weak (weak-amplitude waves), its probability density function can be found by a perturbation technique based on the Gram-Charlier series of type A (Kendall and Stuart 1969), where the coefficients are the statistical moments. The probability density function of the runup of the monochromatic wave with the frequency ω is shown in figure 13 for several values of the parameter B:

$$B = \frac{\omega^2 R_s}{g\alpha^2}, \tag{47}$$

where R_s is the significant wave height on the beach determined as $2\sigma_R$. It is evident from figure 13 that the probability density function becomes asymmetric and shifts towards large values of shoreline displacement with an increase in parameter B.

Thus, in both cases of long-wave runup on a vertical wall and on an inclined beach the nonlinearity increases the probability of rogue wave appearance.

It should be noted again that the process of wave breaking may influence the statistics of the nonlinear wave field. The breaking condition can be found from equation (40):

$$\mathrm{Br} = \max\left[\frac{1}{\alpha g}\frac{\mathrm{d}U}{\mathrm{d}t}\right] = 1, \tag{48}$$

and it is fully determined by the statistical properties of the Gaussian process $U(t)$. Nevertheless, the contribution of the breaking components on the runup characteristics rermains an open problem.

7. Conclusion

The described examples demonstrate that rogue waves can appear in 1D nonlinear hyperbolic systems. This phenomenon is studied here for random shallow-water waves. It is shown that although the nonlinearity in the Riemann wave significantly influences the shape of the wave and leads to the steeping of its face-front, it cannot lead to the extreme wave formation. At the same time the strongly nonlinear Riemann wave cannot be described by the Gaussian statistics (at least, for all components of the wave field). Waves of abnormal height (rogue waves) in nonlinear hyperbolic systems can appear only as a result of nonlinear wave–wave or/and wave–bottom interaction and here we analyse in detail two examples of such interaction: (i) interaction of two Riemann waves moving in opposite directions and (ii) random wave transformation in the basin of variable depth. Although the number of examples, when the probability of rogue wave appearance can be found analytically, is limited, it is obvious that rogue waves exist in nonlinear hyperbolic systems with constant (homogeneous media) and with variable (inhomogeneous media) coefficients.

In 2D and 3D cases the formation of rogue waves becomes even more evident because of the additional space coordinate that allows geometrical focusing of the wave (for example, in KP equation). Nevertheless, analysis of the statistical properties of the nonlinear wave field focusing on rogue wave appearance in such systems has not yet been done and represents an open problem in physics.

Wave breaking (gradient catastrophe), which inevitably occurs in nonlinear hyperbolic systems, should also influence the statistics of rogue wave formation. It is reasonable to assume that wave breaking will reduce the probability of rogue wave formation, since it limits the height of the waves. This influence still stays an open problem, which requires special analysis.

And finally, we should say a few words about dispersive generalizations of nonlinear hyperbolic systems. It has been shown numerically that rogue waves can appear in the random wave field in the framework of KdV and modified Korteweg–de Vries (mKdV) equations (Pelinovsky *et al* 2000, Grimshaw *et al* 2005, Pelinovsky and Sergeeva 2006). Similar effects occur in the framework of KP equation, which is a 2D generalization of KdV equation (Soomere 2010, Yeh *et al* 2010). In all these cases the wave field is considered to be unidirectional or almost unidirectional. At the present moment there are no any studies of rogue wave formation in 1D and 2D nonlinear equations of the Boussinesq type, which also represent an open problem.

Acknowledgments

This research is supported partially by grants from RFBR (11-05-00216), State Contract (02.740.11.0732), Russian President Program (6734.2010.5), and 7th framework programme ‘Extreme Seas’.

References

Akhmediev N, Ankiewicz A and Soto-Crespo J M 2009a Rogue waves and rational solutions of the nonlinear Schrodinger equation *Phys. Rev.* E **80** 026601

Akhmediev N, Ankiewicz A and Taki M 2009b Waves that appear from nowhere and disappear without a trace *Phys. Lett.* A **373** 675–8

Baxevani A and Rychlik I 2006 Maxima for Gaussian seas *Ocean Eng.* **33** 895–911

Carrier G F and Greenspan H P 1958 Water waves of finite amplitude on a sloping beach *J. Fluid Mech.* **4** 97–109

Chien H, Kao C-C and Chuang L Z H 2002 On the characteristics of observed coastal freak waves *Coast. Eng. J.* **44** 301–19

Choi B H, Pelinovsky E, Kim D C, Didenkulova I and Woo S B 2008 Two- and three-dimensional computation of solitary wave runup on non-plane beach *Nonlinear Process. Geophys.* **15** 489–502

Dean R G and Dalrymple R A 2002 *Coastal Processes with Engineering Applications* (Cambridge: Cambridge University Press)

Didenkulova I 2011 Shapes of freak waves in the coastal zone of the Baltic Sea (Tallinn Bay) *Boreal Environ. Res.* **16**

Didenkulova I and Anderson C 2010 Freak waves of different types in the coastal zone of the Baltic Sea *Natural Hazards Earth Syst. Sci.* **10** 2021–9

Didenkulova I and Pelinovsky E 2009 Non-dispersive traveling waves in inclined shallow water channels *Phys. Lett.* A **373** 3883–7

Didenkulova I, Pelinovsky E and Sergeeva A 2011 Statistical characteristics of long waves nearshore *Coast. Eng.* **58** 94–102

Didenkulova I I, Slunyaev A V, Pelinovsky E N and Kharif Ch 2006 Freak Waves in 2005 *Natural Hazards Earth Syst. Sci.* **6** 1007–15

Dyachenko A I and Zakharov V E 2005 Modulational instability of Stokes wave → freak wave *JETP Lett.* **81** 255–9

Dyachenko A I and Zakharov V E 2008 On the formation of freak waves on the surface of deep water *JETP Lett.* **88** 307–11

Dysthe K, Krogstad H E and Muller P 2008 Oceanic rogue waves *Annu. Rev. Fluid Mech.* **40** 287–310

Dysthe K and Trulsen K 1999 Note on breather type solutions of the NLS as a model for freak waves *Phys. Scr.* **T82** 48–52

Engelbrecht J K, Fridman V E and Pelinovsky E N 1988 *Nonlinear Evolution Equations* (*Pitman Research Notes in Mathematics Series No* 180) (London: Longman)

Grimshaw R, Pelinovsky E, Talipova T, Ruderman M and Erdelyi R 2005 Short-lived large-amplitude pulses in the nonlinear long-wave model described by the modified Korteweg–de Vries equation *Stud. Appl. Math.* **114** 189–210

Gurbatov S, Malakhov A and Saichev A 1991 *Nonlinear Random Waves and Turbulence in Nondispersive Media: Waves, Rays and Particles* (Manchester: Manchester University Press)

Kânoğlu U and Synolakis C 2006 Initial value problem solution of nonlinear shallow water-wave equations *Phys. Rev. Lett.* **97** 148501

Kendall M G and Stuart A 1969 *The Advanced Theory of Statistics. vol I. Distribution Theory* (London: Charles Griffin & Co., Ltd) 439pp

Kharif C, Giovanangeli J-P, Touboul J, Grare L and Pelinovsky E 2008 Influence of wind on extreme wave events: experimental and numerical approaches *J. Fluid Mech.* **594** 209–47

Kharif C and Pelinovsky E 2003 Physical mechanisms of the rogue wave phenomenon *Eur. J. Mech.* B **22** 603–34

Kharif Ch, Pelinovsky E and Slunyaev A 2009 *Rogue Waves in the Ocean* (Berlin: Springer) 216pp

Kharif Ch, Pelinovsky E, Talipova T and Slunyaev A 2001 Focusing of nonlinear wave groups in deep water *JETP Lett.* **73** 170–5

Machado U and Rychlik I 2003 Wave statistics in nonlinear random sea *Extremes* **6** 125–46

Onorato M, Osborne A R, Serio M and Bertone S 2001 Freak waves in random oceanic sea states *Phys. Rev. Lett.* **86** 5831–4

Pelinovsky E 1995 Nonlinear hyperbolic equations and runup of huge sea waves *Appl. Anal.* **57** 63–84

Pelinovsky E and Sergeeva (Kokorina) A 2006 Numerical modeling of the KdV random wave field *Eur. J. Mech.* B **25** 425–34

Pelinovsky E, Kharif C and Talipova T 2008 Large-amplitude long wave interaction with a vertical wall *Eur. J. Mech.* B **27** 409–18

Pelinovsky E, Talipova T and Kharif C 2000 Nonlinear dispersive mechanism of the freak wave formation in shallow water *Physica* D **147** 83–94

Peregrine D H 1983 Water waves, nonlinear Schrodinger equations and their solutions *J. Aust. Math. Soc.* B **25** 16–43

Pomeau Y, Le Berre M, Guyenne P and Grilli S 2008 Wave-breaking and generic singularities of nonlinear hyperbolic equations *Nonlinearity* **21** T61–T79

Ruban V *et al* 2010 Rogue waves—towards a unifying concept? Discussions and debates *Eur. Phys. J. Spec. Top.* **185** 5–15

Rudenko O and Soluyan S 1977 *Theoretical Background of Nonlinear Acoustics* (New York: Plenum)

Slunyaev A V 2009 Numerical simulation of 'limiting' envelope solitons of gravity waves on deep water *JETP* **109** 676–86

Solli D R, Rogers C, Koonath P and Jalali B 2007 Optical rogue waves *Nature* **450** 1054–7

Soomere T 2010 Rogue waves in shallow water *Eur. Phys. J. Spec. Top.* **185** 81–96

Stoker J J 1957 *Water Waves* (New York: Willey-Interscience)

Synolakis C E 1987 The runup of solitary waves *J. Fluid Mech.* **185** 523–45

Voronovich V V, Shrira V I and Thomas G 2008 Can bottom friction suppress 'freak wave' formation? *J. Fluid Mech.* **604** 263–96

Yeh H, Li W and Kodama Y 2010 Mach reflection and KP solitons in shallow water *Eur. Phys. J. Spec. Top.* **185** 97–111

Zahibo N, Didenkulova I, Kurkin A and Pelinovsky E 2008 Steepness and spectrum of nonlinear deformed shallow water wave *Ocean Eng.* **35** 47–52

Zahibo N, Pelinovsky E, Golinko V and Osipenko N 2006 Tsunami wave runup on coasts of narrow bays *Int. J. Fluid Mech. Res.* **33** 106–18

Zakharov V E and Ostrovsky L A 2009 Modulation instability: the beginning *Physica* D **238** 540–8